Reynolds Averaged Radiative Transfer Model

Carl A. Svoboda

School of Mathematical and Physical Sciences
Department of Mathematics and Statistics

This dissertation is for a joint MSc in the Departments of Mathematics & Meteorology and is submitted in partial fulfilment of the requirements for the degree of Master of Science

26 August 2011

Declaration

I con rm that this is my own work and the use of all material from other sources has been properly and fully acknowledged.

Signed .....

Acknowledgements

I would like to thank my supervisor Dr Robin Hogan for his continued dedication and support towards this preoject. I would also like to thank Dr Peter Sweby and the Natural Environment Research Council for giving me the opportunity and funding to undertake this MSc.

Abstract

In order for accurate predictions of climate change, it is essential that radiative transfer processes within the atmosphere are represented accurately in GCMs. The Radiative Transfer component of climate models is one of the 'rate-limiting' areas in the computation (Natraja *et al.*, 2005). While several techniques have been proposed to speed up radiative transfer calculations, they all su er from accuracy considerations (Natraja *et al.*, 2005). A review of current techniques used within radiative transfer modelling is given followed by the development of a new, Reyolds averaged radiative transfer model. Starting with a simple case, reducing the radiative transfer equation (RTE) to exclude scattering and emission. The uctuating terms within the RTE are Reynolds decomposed and a system of linear, homogeneous di erential equations is solved involving a closure problem, which requires parameterization. Real atmospheric absortion spectra are used and an accuracy of 10^{6} Wm^{2} is achieved for 100 bands in an equal weighted band model, where each band has the same number of extinction coe cients within it. The models developed have di culty in representing a large range of absorption coe cient. The next step in the development and testing of a Reynolds averaged radiative transfer model would be to include radiation travelling in di erent directions and to also include emission along the path, therefore having to include the Planck function. Then we would like to account for scattering. We would also like to account for an inhomogeneous path, where pressure and temperature change.

Contents

List of Figures

List of Tables

Chapter 1

gases and clouds. These processes have a strong impact on the surface energy balance (Ritter & Geleyn, 1992).

As in many areas of numerical modelling, especially in GCMs, it is desirable for the mathematics within the model to be calculated quickly, whilst describing as accurately as possible the interaction of radiative processes (Ritter & Geleyn, 1992) (Dessler *et al.*, 1996) as even a change of 1% in radiation calculations are signi cant for climate (Turner *et al.*, 2004).

At present, large computational resources are required for the calculation of radiative transfer in the atmosphere for weather and climate prediction (Fomin, 2004). The radiative transfer component of climate models is one of the 'rate-limiting' areas in the computation (Natraja *et al.*, 2005). While several techniques, which will be discussed later, have been proposed to speed up radiative transfer calculations, they all su er from accuracy considerations (Natraja *et al.*, 2005). The need to improve the computational e ciency of the numerical models causes the problem of gaining the right balance between e ciency and accuracy (Stephens, 1984). Radiative transfer schemes will have to compromise between these two criteria (Ritter & Geleyn, 1992).

As full treatment of the radiative transfer code in GCMs, incorporating all known physics is computationally expensive, parameterization is required (Turner *et al.*, 2004). The cost e ectiveness of a parameterization scheme is subject to many in uences. First there is the solution method to the radiative transfer equation (RTE) and the approximation associated with it. Second there is the number of intervals used to resolve the spectrum. Further economy can be achieved in many models by considering only those optical constituents of the atmosphere that are important in a particular spectral domain. Often some atmospheric constituents in certain spectral intervals are neglected where their impact is well below that of other constituents (Ritter & Geleyn, 1992).

As an example of the importance in obtaining code accurate enough to model these atmospheric interactions, there are large di erences among recent GCM simulations for prescribed changes in stratospheric water vapour (stratospheric water vapour being an important contributor to the observed stratospheric cool-

ing); this points to problems with the current GCM treatment of the absorption and emission by stratospheric water vapour (Oinas *et al.*, 2001).

Even considering the current computational efficiency of radiation calculations in numerical weather prediction models and GCMs, these models still require substantial computational time relative to all other physical and dynamical calculations. As a result, radiation subroutines in these models are usually not called as often as would be desired, even being called less often than the time scale on which clouds evolve in the models. High spectral accuracy is therefore

transfer equation and applying Reynolds averaging to the variables which vary with wavelength. The main aims will be:

Determine the accuracy of a simpli ed situation, no scattering or emission and with radiation travelling in only one direction.

Investigate how the standard deviation, of the absorption coe cients a ects the accuracy of the scheme

Investigate the number of quadtratue points required to acheive desired accuracy

Investigate if bands are bands still required

Total number of bands

How best to de ne the bands

Add emmission, planck function into equations

A di usivity fator, for radiation travelling in di erent directions

Chapter two will give an overview of the science background required to fully understand the processes within the model. Chapter three gives a summary of current techniques used to treat the complicated absorption spectrum. Chapter four gives the derivation of the equations used within the model and a description of how the model works. Chapter ve presents some results from the model and chapter six discusses these results.

Chapter 2

Scientific Background

The radiative transfer process is essentially the process of interactions between matter and a radiation field (Fu & Liou, 1992). Thermal Infra Red (IR) radiation is the most important factor when considering the distribution of heat within the atmosphere. IR radiation is emitted from the Earth and the atmosphere.

temperature of the Earth's atmosphere. Hence IR radiation and the amounts absorbed and re-emitted within the atmosphere play a major role in quantifying future climate change (Liou, 1992).

2.1 Emission

The Earth and the atmosphere are continuously emitting IR radiation which may be radiated out into space or may be absorbed by other parts of the atmosphere. The emission of an object is directly related to the temperature of that object. An object of temperature T will emit over all possible wavelengths. The relationship between, temperature, wavelength and the amount of radiation emitted is de ned by the Planck Function (2.1) (Petty, 2004):

$$B\ (T) = \frac{2hc^2}{^5(e^{hc=k_B\ \ T}\quad 1)}; \tag{2.1}$$

where c=2.988 10^8 m s ^{1}, (the speed of light), h=6.626 10 ^{34} J s represents Planck's constant and k_B=1.381 10 ^{23} J K ^{1} represents the Boltzmann's constant.

Figure (2.1) shows the shape of the Planck Function for several atmospheric temperatures. The curves describe the maximum amount of thermal radiation a body could emit, thus describing a 'black body' (one which absorbs and emits all radiation incident upon it) (Petty, 2004).

For any temperature there will be a speci c wavelength at which there occurs a maximum in the amount of radiation emitted. This wavelength is de ned by Wien's Displacement Law (2.2) (Petty, 2004):

$$_{max} = \frac{C}{T}; \tag{2.2}$$

where $_{max}$ is the wavelength at which the peak in emission occurs and C=2897 m K.

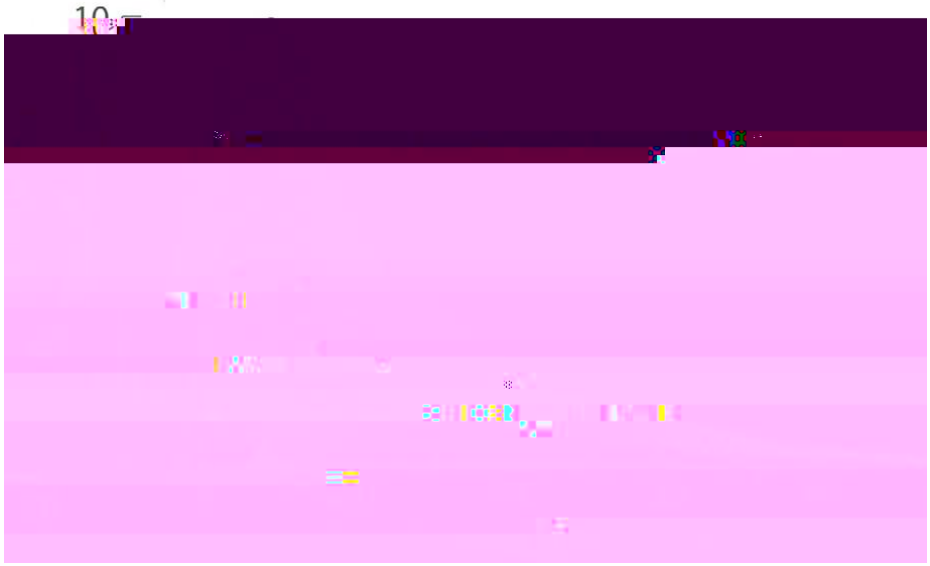

Figure 2.1: The Planck Function B for Blackbodies at typical atmospheric temperatures (Petty, 2004).

Equation (2.2) shows that the warmer the object, the shorter the wavelength at which the peak in emission occurs. If Planck's Function is integrated over all wavelengths we obtain Stefan-Boltzmann Law (2.4), which quanti es the total amount of radiation which can be emitted from a perfect black body (the blackbody ux F_{BB}) (Petty, 2004):

$$F_{BB}(T) = \int_0^1 B\ (T)d\ ; \tag{2.3}$$

$$F_{BB}(T) = \ T^4; \tag{2.4}$$

where = 5:67 10 ^{8} Wm ^{2}K ^{4}.

2.2 Absorption and Scattering

We can de ne the extinction coe cient $_e$ (2.5) as the sum of the extinction due to absorption $_a$ and the extinction due to scattering $_s$ (Petty, 2004).

$$_e = _a + _s: \tag{2.5}$$

We are now able to de ne the single scatter albedo $\dot{}$ (2.6), which de nes the relative importance of scattering and absorption. $\dot{}$ ranges from 0 for purely absorbing mediums to 1 for purely scattering material (Petty, 2004):

$$\dot{} = \quad snat] [(( ) .955 \ 48955914 \ 727.757 \ cm[]0 \ 7 \ 0 \ J \ 0.498.95525m \ 41$$

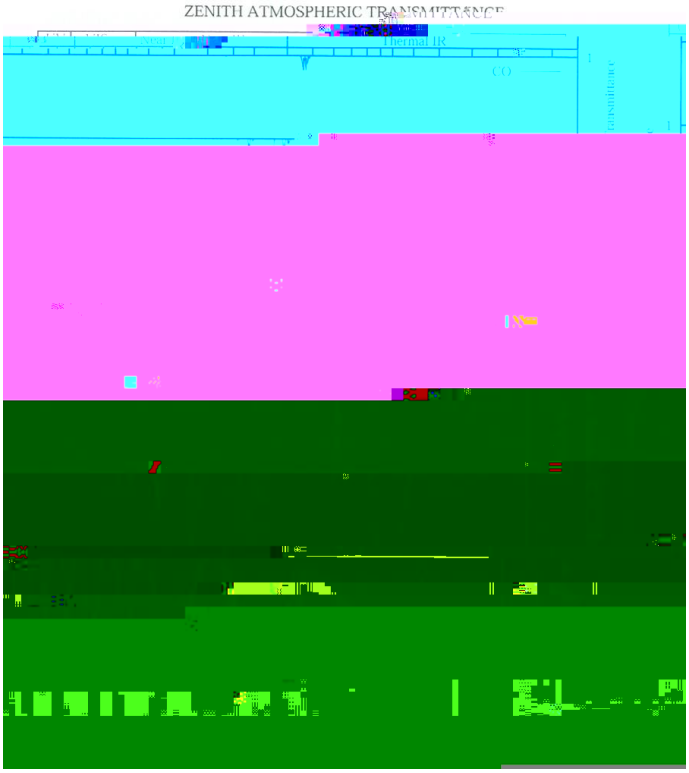

Figure 2.2: The zenith transmittance of a cloud and aerosol free atmosphere for a mid latitude summertime. The bottom panel depicts the combined e ect of all the constituents above (Petty, 2004).

The most important absorbers are carbon dioxide (CO

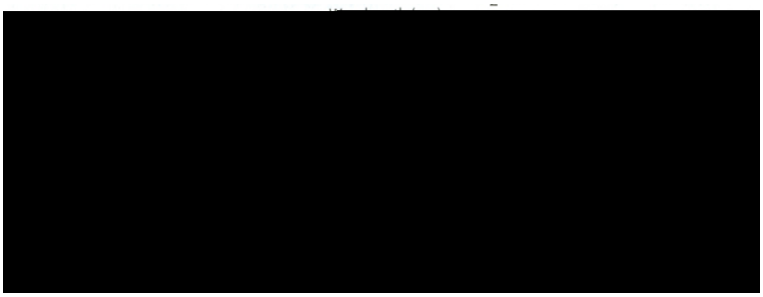

Figure 2.3: The zenith transmittance of the atmosphere due to water vapour in the thermal IR (Petty, 2004).

The x-axis is measured in wavenumber ν, which is simply the reciprocal of the wavelength (2.7) and therefore its units are in cm ^{1}.

$$\nu = \frac{1}{\lambda}: \tag{2.7}$$

The absorption spectrum of water vapour exhibits great complexity and if one were to zoom in on gure (2.3), it would become apparent that the complexity exists on wave length scales up to 10 ^{4} cm ^{1}. At wavelengths greater than 25 m the atmosphere is more or less opaque with regards to H_2O absorption (Liou, 1992).

2.3 Radiative Transfer Equation

We are interested in the amount of radiation travelling through a part of the atmosphere. As the electromagnetic (EM) radiation transports energy, we quantify the amount of radiation transferred with power, using the Watt, W (the amount of energy measured in Joules, J, per unit time, s) (Petty, 2004). It is common to refer to the amount of radiation received in terms of its ux density F, the rate of energy transfer per unit area Wm ^{2}. From here on in ux shall be used to refer to ux density. The ux is the rate at which the radiation passes through a at surface including all wavelengths between a speci ed range (Petty, 2004).

We shall consider how EM radiation is e ected when it travels along a path of homogeneous medium and is able to be absorbed by the medium. The intensity or radiance tells us about the strength and direction of the various sources which contribute to the ux.

The ux passing through the surface will be the integral of intensity over all the possible directions from which the radiation is incident. As only one direction is normal to the surface, all contributions from other directions must be weighted by the cosine of the incident angle relative to the normal. So in spherical polar coordinates the relationship between ux and intensity can be written (Petty, 2004),

$$F = \int_0^{2} \int_0^{=2} I(\; ; \;) \cos \sin \, d \, d \; ; \tag{2.8}$$

where $I(\; ; \;)$ is the irradiance over all possible incident angles. We shall now consider the absorption of a monochromatic EM wave propagating through a homogeneous atmosphere. The most simple governing equation for this occurs where the wave is travelling in one direction only and is attenuated only by absorption (Petty, 2004),

$$dI \; (z) = \; {}_a I \; {}_{;0} dz; \tag{2.9}$$

where ${}_a$ is the absorption coe cient, which depends on the physical medium and the wavelength of the radiation, I (z) is the intensity of the transmitted radiation at some distance, z, and I ${}_{;0}$ is the intensity of the radiation at z=0. We can rearrange and integrate (2.9) over the range of intensities and the distance the radiation travels to obtain (Petty, 2004):

$$I \; = I \; {}_{;0} \exp(\; {}_a z):$$

atmosphere. The beam of radiation is not only attenuated by absorption, but also by scattering due to interactions with particles. We can now use our previously de ned extinction coe cient in place of the absorption coe cient to account for scattering. We consider our beam of radiation over a nite path where extinction coe cient varies with location. We replace the height, z, by s to represent a distance in any direction, represented by g. (2.4).

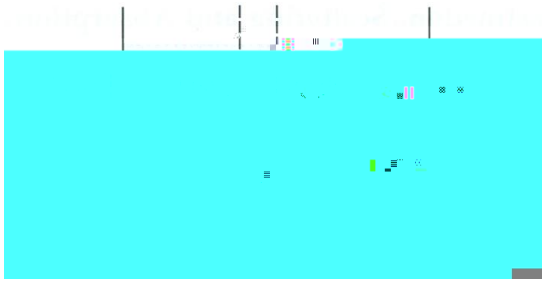

Figure 2.4: Depletion of radiation over an in nitesimal path ds (Petty, 2004)

If ds is considered to be in nitesimal, then the extinction coe cient $_e$ will be constant within the interval. The radiation will then change by an in nitesimal amount dI and we can re-write (2.9) to include loss due to scattering, however no gain from scattering:

$$dI\ (s) = \quad I\ (s)\ _e(s)ds: \tag{2.11}$$

We can consider the amount of radiation attenuated due to absorption only by writing (2.12) (Petty, 2004)

$$dI_{abs} = \quad I\ _a ds: \tag{2.12}$$

Neglecting scattering ($_a$ = $_e$), we know from Kircho 's law discussed earlier that the absorptivity of any material is equal to the emissivity of that material. We can therefore de ne the amount of radiation that the thin layer of air will

emit by (2.13) (Petty, 2004):

$$dI_{emit} = B\ (T)\ {}_a ds; \tag{2.13}$$

enabling us to de ne Schwarzschild's Equation (2.14), the net change in radiation over the in nitesimal path in a non scattering medium (Petty, 2004):

$$dI = dI_{abs} + dI_{emit} = {}_a(B \quad I)ds: \tag{2.14}$$

We are now ready to include scattering into our radiative transfer equation. Now we have

$$dI_{ext} = \quad {}_{ext} I ds: \tag{2.15}$$

We must consider one more process to complete the RTE, in considering a new source term which includes the contributions to the beam as a result of scattering from other directions. We shall call this new source term, dI_{scat}. This term will be pro portional to the scattering coe cient ${}_s$. We can de ne the direction of travel we are interested in $\hat{}$ and we can state that any radiation from any direction emit(de ned by $\hat{}\,'$

We can divide through by the change in optical thickness d and can then write the complete form of the RTE (2.18) (Petty, 2004)

$$\frac{dI(\hat{})}{d} = \quad I(\hat{}) + (1 \quad \dot{\iota})B + \frac{\dot{\iota}}{4}\int_{4} p(\hat{}^{0};\hat{})I(\hat{}^{0})d!^{0}: \qquad (2.18)$$

2.4 Reynolds Decomposition

Figure (2.3) of the absorption spectrum for water vapour in the thermal IR is very remeniscent of a turbulence spectrum observed in many other areas of the atmosphere, such as the variation in surface wind speed over a certain amount of time. The transmittance due to water vapour appears to vary randomly across wavelengths, however the ability to nd a mean value suggests that the spectrum is not random.

We can average the transmittance spectrum over a certain, number of intervals, averaging out the positive and negative uctuatios about the mean. The mean transmittance in one interval is denoted, $\overline{T}$. At any one particular wavelength, we can subtract $\overline{T}$ from the actual transmittance, T, which will result in the uctuating part, T^{0}. This is represented schematically in gure (2.5) which

Figure 2.5: The deviation, T^0 of the actual, transmittance, T, from the local mean, $\overline{T}$

2.5 Reynolds Averaging Rules

If we let A and B be two variables that are dependent on the wavelength. We can show some rules using integration.

2.5.1 Rule One

The average of a sum (Stull, 1989):

$$\overline{A+B} = \frac{1}{N}\int_{Z=0}^{N}(A+B)\,d \tag{2.20}$$

$$= \frac{1}{N}\int A\,d + \int B\,d \tag{2.21}$$

$$= \frac{1}{N}\int A\,d + \frac{1}{N}\int B\,d \tag{2.22}$$

$$= \overline{A}+\overline{B} \tag{2.23}$$

2.5.2 Rule Two

An average value acts as a constant, when averaged a second time over the same wavelength interval (Stull, 1989).

$$\frac{1}{N}\int_{=0}^{N} A\,d = \overline{A}$$

The only way the above can be true is if,

$$\overline{A''} = 0. \tag{2.33}$$

This makes sense as the sum of the positive deviations from the mean must equal the sum of the negative deviations from the mean.

2.5.5 Rule Five

Chapter 3

Literature Review

As already seen, atmospheric gases have absorption coe cients that vary rapidly as a function of wavelength or wave number v, often changing by several orders of magnitude across the electromagnetic spectrum (Petty, 2004). This provides a great problem when the absorption spectra are modelled in GCMs, as there can be $O(10^5)$ individual absorption lines within the spectrum. If we were to model each individual line, large amounts of computer power would be required to calculate the uxes in the atmosphere (Ellingson *et al.*, 1991). Here we shall discuss some of the techniques developed to overcome this problem and reduce the time taken for the models to run, increasing the computational e ciency, whilst attempting to maintain a suitable degree of accuracy.

3.1 Line by Line Calculations

Absorption occurring at the smallest scale, that of the line, is described by the Lorenz line absorption pro le. The most straightforward and accurate but most computationally expensive way to perform radiative transfer calculations is to divide the full spectrum into monochromatic (one wavelength) intervals, or su - ciently small so as to be treated as monochromatic (10^{-4} to 10^{-2} cm $^{-1}$) (Ellingson *et al.*, 1991). The relative contributions of all relevant absorption lines (all lines whose wings contribute to important absorption at a particular wavelength)

are summed to the absorption coe cient, $_a$, for the wave number in question (Petty, 2004). Integrating over all intervals in the spectrum then provides uxes and heating rates (Ellingson *et al.*, 1991). This however is not a simple task. The absorption spectrum depends on many things, including the location, strengths and shapes of the spectral lines (Ellingson *et al.*, 1991).

A LBL calculation of the average transmittance of a spectral interval (v_1 v_2) over a nite mass path, u, can be calculated by considering (Petty, 2004):

$$T(u) = \frac{1}{v_2 \quad v_1} \int_{v_1}^{v_2} \exp[\quad k(v)u]dv; \tag{3.1}$$

which can be approximated as a sum:

$$T(u) = \sum_{i=1}^{N} {}_i \exp[\quad k(v)u]; \tag{3.2}$$

where N is the number of frequencies, v_i, where $k(v)$ is evaluated and $_i$ are weighting coe cients depending on the quadtrature method used.

Because the technique involves summing the contributions from each spectral line, it is referred to as the Line-By-Line technique (LBL) (Ellingson *et al.*, 1991). If this approach was to be used to calculate heating rates in the atmosphere, the monochromatic calculation would need to be repeated for a large number of wavenumbers as well as at a number of altitudes (Petty, 2004). This means that radiative heating calculations potentially require millions of calculations to obtain a suitable accuracy (Pawlak *et al.*, 2004). Where eld measurements are unavailable, LBL techniques provide the best benchmark for analysis of other numerical methods (Ellingson *et al.*, 1991Ele-32381ty, 2004). This means

678uOne3 T0Ele-1r407.proxima407.9s3 T0p accuratinga59

3.2 Band Models

Due to the difficulty and computational demands of treating a single Lorenz line individually, the idea of the band model was developed, which enables certain characteristics of the band to be determined using simple statistical relationships, such as, averaging of the absorption properties (Petty, 2004). An analytic approximation for the transmittance is then derived. (Stephens, 1984) suggests that the most widely used in atmospheric flux calculations is that of Goody (1952) where the absorbing lines are assumed to be randomly distributed.

3.3 k-distribution Method

3.3.1 k-distribution Method Theory

This method was first discussed by Ambartzumin (1936). It aims to perform the radiative calculations with larger discretisations by replacing the complex integration over wavenumber with an equivalent integration over a much smoother function (Petty, 2004) and involves grouping spectral intervals according to absorption coefficient strength (Natraja *et al.*, 2005). The absorption coefficient across a portion of the spectrum can be reordered into a monotonically increasing function called the k-distribution function (Modest & Zhang, 2002).

When the k-distribution method is used within a narrow band model, the longwave spectrum $k(\nu)$, is divided into N intervals ν_i, each having a smaller range of $k(\nu)$ values (Mlawer *et al.*, 1995). This procedure treats each subinterval in an equivalent manner as a spectral point is treated in a monochromatic radiative transfer method (Mlawer *et al.*, 1997). The division of these intervals is determined by the fact that they must be large enough to contain a significant amount of absorption lines associated with a particular absorber and also, they must be small enough so that the Planck function $B_\nu(T)$ can be treated as constant and equal to $\overline{B}_i$ across the band (Petty, 2004). The creation of the k-distribution involves assigning each absorption coefficient $k(\nu)$ a value g (0-1) that represents the fraction of the absorption coefficients in the band smaller than the representative $k(\nu)$. The k-values are re-arranged into ascending order transforming the spectrum into a smooth monotonically increasing function of the absorption coefficient, representing a cumulative k-distribution, g, defining a mapping, ν - g (Mlawer *et al.*, 1995). This can be seen in figure (3.1), which shows one such mapping, where the absorption coefficients for the spectral range (30-700 cm ^{1}) undergo a transformation into g-space figure (3.1b). The effect of this reordering is simply a rearrangement of the sequence of terms in the integral over wavenumber in the radiative transfer equations (Mlawer *et al.*, 1997).

By integrating over $k(g)$ instead of the complicated $k(\nu)$ we can replace the

3.4 Correlated k-distribution Method

3.4.1 Correlated k theory

The k-distribution method discussed above assumes a homogeneous path (one over which the temperature and pressure remain the same). This means the method would only suit very short paths through the atmosphere. This led to an extension of the k-distribution method to account for vertical paths in the

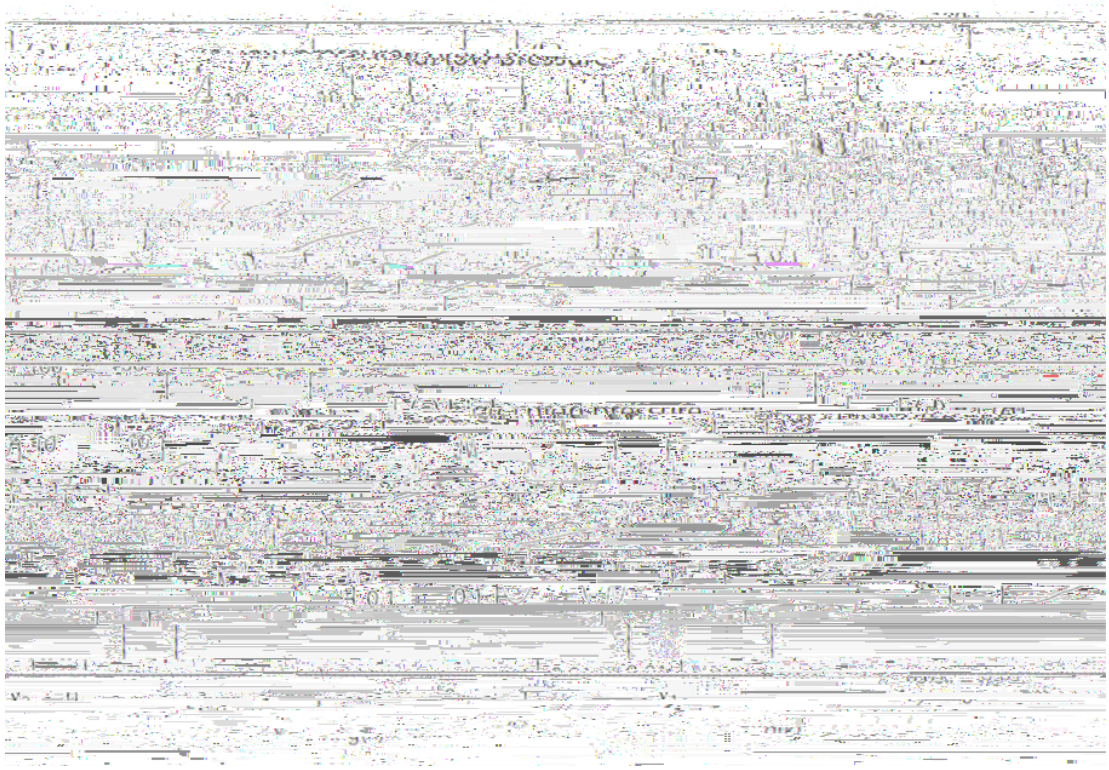

Figure 3.2: The k-distribution method and its extension to the correlated k method. (a) Absorption spectrum at low pressure, (b) sorting k to increase monotonically to form the function $g(k)$. (c) the same as for a and b, however at higher pressure, so are e ected by pressure broadening (Petty, 2004)

mogeneous path (Petty, 2004).

$$T(u) = \int_0^1 \exp\left[\int_0^u k(g;u')du'\right] dg. \tag{3.4}$$

This equation calculates the transmittance for a speci c value of gu

di erent frequencies. This can be seen in (3.2), the horizontal dotted line corresponds to a single value of k, yet has many values of frequency associated with it. In the CK Method, the absorption coe cient at all of these frequencies is associated to a single value of g (depicted by the intersection of the dotted line with the $k(g)$ curve gure (3.2b)).

Figure (3.2c) shows the absorption spectrum for a level higher in the atmosphere and its corresponding $k(g)$ mapping is represented in gure (3.2d). The absorption spectrum is a ected by pressure broadening leading to a smoother spectrum with less extreme values of k. As a result, the spectral elements that contribute to a subinterval of the k-distribution for one homogeneous layer will not be mapped to the corresponding subinterval for a di erent atmospheric layer (Mlawer *et al.*, 1997). This leads to a di erent $k(g)$ distribution at the higher pressure. The newly determined frequencies at higher pressure, determined by the choice of k at lower pressure are not far o those frequencies at the lower pressure and this method does provide results within accuracy restraints.

The CKD method overestimates and underestimates the absorption in the vicinity of maximum and minima respectively. As a result, the CKD method may overestimate the spectral mean transmittance, leading to a more transparent atmosphere (Fu & Liou, 1992). The method does calculate uxes and heating rates to errors of less than 1% (Petty, 2004) and is three orders of magnitude less computational power is required than LBL calculations (Petty, 2004).

3.5 Rapid Radiative Transfer Model (RRTM)

RRTM stands for the Rapid Radiative Transfer Model (Clough *et al.*, 2005). Modelled molecular absorbers are water vapour, carbon dioxide, ozone, nitrous oxide, methane, oxygen, nitrogen, and halocarbons. The model is accurate and fast, using the correlated-k method in its computation. RRTM divides the LW spectral region into 16 bands chosen for their homogeneity and radiative transfer properties (Mlawer *et al.*, 1995) (Clough *et al.*, 2005). There are a number of areas which can be explored to improve the speed of the model. The number

of subintervals into which some of the bands are divided could be reduced and combining separate spectral regions which have similar absorbing properties into single spectral bands could help reduce the time taken for the model to run (Mlawer *et al.*, 1997).

(Fu & Liou, 1992) explored the optimum number of g values suitable within each band. They found that the number of quadrature points to provide sufficient accuracy could vary from 1 (for weak absorbing bands) to 10 (for strong absorption bands).

Each spectral band in the RRTM is broken into 16 intervals with 7 intervals lying between $g = 0.98$ and $g = 1.0$. This modified quadrature spacing is done to better determine the cooling rate where high values of $k(g)$ are associated with the centres of the spectral lines in the band (Mlawer *et al.*, 1995). The k-distribution is divided into subintervals of decreasing size with respect to g, with high resolution towards the upper end of the distribution. This arrangement allows accurate determination of middle atmosphere cooling rates while preserving the speed of the model (Mlawer *et al.*, 1997). At different atmospheric levels there is a limited range of absorption coefficient values that provide the main contribution to the cooling rate. Therefore when g approaches 1, only a small fraction of the k-distribution will have contributed due to the rapid increase in the function $k(g)$ at the high end of the distribution, which is why a high resolution is required near $g=1$ (Mlawer *et al.*, 1997). This high resolution in space near $g=1$ is difficult to achieve while maintaining speed of execution.

(Mlawer *et al.*, 1997) considers three main points when determining the number of spectral bands to use in RRTM:

Each spectral band can have at most two species with substantial absorption.

The range of values of the Planck function in each band cannot be extreme.

The number of bands should be minimal.

An absorbing gas which dominates the absorption within a certain spectral band is termed a 'key species' and it is treated in more detail than other species in the bands that have smaller but still important absorption. These are referred to as 'minor species'. Table 3.1 presents the spectral bands of RRTM in the LW region (Mlawer *et al.*, 1997).

Band Number	Wavenumber Range, cm_1	Species Implemented in RRTM			
		Lower Atmosphere		Middle/Upper Atmosphere	
		Key Species	Minor Species	Key Species	Minor Species
1	10-250	H_2O		H_2O	
2	250-500	H_2O		H_2O	
3	500-630	H_2O, CO_2		H_2O, CO_2	
4	630-700	H_2O, CO_2		13.65, O_3	
5	700-820	H_2O, CO_2	CCl_4	CO_2, O_3	CCl_4
6	820-980	H_2O	CO_2, CFC-11, CFC-12	...	CFC-11, CFC-12
7	980-1080	H_2O, O_3	CO_2	O_3	
8	1080-1180	H_2O	CO_2, CFC-12, CFC-22	O_3	
9	1180-1390	H_2O, CH_4		CH_4	
10	1390-1480	H_2O		H_2O	
11	1480-1800	H_2O		H_2O	
12	1800-2080	H_2O, CO_2		...	
13	2080-2250	H_2O, N_2O		...	
14	2250-2380	CO_2		13.65	
15	2380-2600	CO_2, N_2O		...	
16	2600-3000	H_2O, CH_4		...	

Table 3.1: RRTM Bands (Mlawer *et al.*, 1997)

3.5.1 Accuracy

The LW accuracy of RRTM is 0.6 Wm ^{2} (relative to the LBLRTM) for the net ux in each band at all altitudes with a total error of less than 1.0 Wm ^{2} at any altitude. It recorded an error of 0.07 K d ^{1} for total cooling rate error in the troposphere and lower stratosphere and 0 .75 K d ^{1} in the upper stratosphere (Mlawer *et al.*, 1997).

Results of timing tests for RRTM indicate that computing the uxes and cooling rates for a 51-layer atmosphere which includes the performance of 256 (16 bands x 16 subintervals) upward and downward radiative transfer calculations and, therefore, the computation of 256 optical depths per layer, takes 0.06 s on a SPARC server 1000. This compares favourably with the other rapid radiative transfer models (Mlawer *et al.*, 1995). A further indication of the computational e ciency of the model is that these radiative transfer operations in RRTM take 1.8 times the amount of time needed to perform 51 x 16 x 16 exponentials. The speed and the accuracy of this model makes it suitable for use in GCMs (Mlawer *et al.*, 1997).

3.6 Full-Spectrum Correlated k-distribution Method (FSCK)

3.6.1 FSCK Method theory

The full-spectrum correlated-k distribution method (FSCK) is similar to the correlated k-distribution method (Li & Modest, 2002). In the FSCK method the absorption coe cients, k, are again sorted into smooth, monotonically increasing cumulative k-distributions, which enables the spectrum to be calculated with fewer calculations. The correlated k-distribution method is limited by the fact that the Planck function must be constant over the spectral range of the absorption coe cients. In the FSCK method, there is no restriction on the Planck function eliminating the need for a constant Planck function across each spectral

region (Pawlak *et al.*, 2004). As a result, in the FSCK approach, spectral bands can now be large, even as big as the full spectrum (Pawlak *et al.*, 2004).

Note that to eliminate the requirement that the Planck function must be constant over the spectral interval being sorted, the k-distribution is rede ned using the Planck function as a weighting function. This means that the k-distribution gains temperature dependence through the Planck function (Pawlak *et al.*, 2004). (Stull, 1989) showed that an e ective Planck function (the integral of the Planck function over wavenumbers which contribute to absorption in a particular range of g) can be used to replace the Planck function in the radiative transfer equations.

By eliminating the necessity for multiple spectral bands, the total number of calculations can be reduced substantially without losing signi cant accuracy relative to LBL calculations (Pawlak *et al.*, 2004).

Since FSCK requires quadrature over a single monotonically increasing function and needs about 10 quadrature points, while LBL calculations require about 1 million quadrature points, the FSCK method will greatly speed up the calculations. (Modest & Zhang, 2002) states that FSCK calculations required less than 0.05 seconds to perform de ned calculations while the LBL calculations required 25 minutes.

Chapter 4

Method

4.1 Complex Radiative Tr8nm=hapter 4

$$dF = d\overline{F} + dF' \tag{4.6a}$$
$$= \overline{\ } + \ ' \tag{4.6b}$$
$$F = \overline{F} + F' \tag{4.6c}$$
$$B = \overline{B} + B' \tag{4.6d}$$

We begin by taking (4.5) and substituting into it the Reynolds decomposed versions of the variables found in (4.6):

$$d\overline{F} + dF' = D \ \overline{\ } + \ ' \quad \overline{F} + F' \quad \overline{B} \quad B' \ dz: \tag{4.7}$$

We can then multiply out the brackets:

$$d\overline{F} + dF' = D \ \overline{\ }\,\overline{F} + \overline{\ }F' \quad \overline{\ }\,\overline{B} \quad \overline{\ }B' + \ '\overline{F} + \ 'F' \quad \ '\overline{B} \quad \ 'B' \ dz: \tag{4.8}$$

We now average over the whole spectrum, using rules 4, 5 and 6 from section 2.5, so any term with only one prime will cancel leaving

$$d\overline{F} = D \ \overline{\ }\,\overline{F} \quad \overline{\ }\,\overline{B} + \overline{\ 'F'} \quad \overline{\ 'B'} \ dz \tag{4.9}$$

This equation contains a covariance term which in principle we know $\overline{\ 'B'}$, the covariance of the known spectral variation of the Planck Function with the known variation of the absorption coe cient.

the equation also contains a term we do not know $\overline{\ 'F'}$. We can derive an expression for it by subtracting equation (4.9) from (4.8)

$$d\overline{F} + dF' \quad d\overline{F} = \quad D \ \overline{\ }\,\overline{F} + \overline{\ }F' \quad \overline{\ }\,\overline{B} \quad \overline{\ }B' + \ '\overline{F} + \ 'F' \quad \ '\overline{B} \quad \ 'B' \ dz$$
$$+ \ D \ \overline{\ }\,\overline{F} \quad \overline{\ }\,\overline{B} + \overline{\ 'F'} \quad \overline{\ 'B'} \ dz: \ (:)]TJ \ 0.8$$

4.5

$$dF^{'} = \quad D \quad + \bar{} F^{'} \quad \bar{} B^{'} + \quad {}^{'}\overline{F} + \quad {}^{'}F^{'} \qquad {}^{'}\overline{B} \qquad {}^{'}B^{'} \qquad \overline{{}^{'}F^{'}} + \overline{{}^{'}B^{'}} \; dz: \tag{4.11}$$

We want an equaiton for $d\overline{{}^{'}F^{'}}$ to predict $\overline{{}^{'}F^{'}}$. Using the chain rule we can expand $d\overline{{}^{'}F^{'}}$

$$d\overline{{}^{'}F^{'}} = \overline{{}^{'}dF^{'}} + \overline{F^{'}d \quad {}^{'}}: \tag{4.12}$$

We are treating the extinction coe cient as constant along a path so $d \quad {}^{'} = 0$

$$d\overline{{}^{'}F^{'}} = \overline{{}^{'}dF^{'}}: \tag{4.13}$$

We can now times (4.11) by $\quad {}^{'}$ and take the average over the spectrum.

$$\overline{{}^{'}dF^{'}} = d\overline{{}^{'}F^{'}} = \quad D \quad \bar{} \; \overline{{}^{'}F^{'}} \qquad \bar{} \; \overline{{}^{'}B^{'}} + \overline{{}^{'2}}\,\overline{F} \qquad \overline{{}^{'2}}\,\overline{B} \qquad \overline{{}^{'2}F^{'}} \qquad \overline{{}^{'2}B^{'}} \; dz: \tag{4.14}$$

The last two terms in (4.11) disappear when the average is taken and we obtain (4.14) which again contains an unknown, this time of a higher order $\overline{{}^{'2}F^{'}}$

We can follow the same procedure again to obtain an equation for the new unknown.

$$d\overline{{}^{'2}F^{'}} = \overline{{}^{'2}dF^{'}} = \quad D \quad \overline{{}^{'3}\,F^{'}} \qquad \overline{{}^{'3}}\,\overline{B} + \bar{} \; \overline{{}^{'2}F^{'}} \qquad \bar{} \; \overline{{}^{'2}B^{'}} + \overline{{}^{'3}F^{'}} \qquad \overline{{}^{'3}B^{'}} \; dz: \tag{4.15}$$

Now we again have another unknown this time of higher order $\overline{{}^{'3}B^{'}}$ again this is a closure problem. We could keep on deriving equations for the unknowns, however, each time we derive a new equation, it will have a new unknown of one higher order than that of the term we are trying to derive. This is known as the closure problem Stull (1989). We overcome this problem, by parameterizing the unknown term at a certain stage where we require a certain accuracy.

So up to third order accuracy we can de ne F by these three equations

$$\frac{d\overline{F}}{dz} = D(\overline{\ } \overline{F} \quad \overline{\ } \overline{B} + \overline{{}^{0}F^{0}} + \overline{{}^{0}B^{0}}+) \tag{4.16a}$$

$$\frac{d\overline{{}^{0}F^{0}}}{dz} = D(\overline{{}^{0^2}}\,\overline{F} \quad \overline{{}^{0^2}}\,\overline{B} + \overline{\ }\,\overline{{}^{0}F^{0}} + \overline{{}^{0^2}F^{0}} \quad \overline{\ }\,\overline{{}^{0}B^{0}} \quad \overline{{}^{0^2}B^{0}}) \tag{4.16b}$$

$$\frac{d\overline{{}^{0^2}F^{0}}}{dz} = D(\overline{{}^{0^3}}\,\overline{F} \quad \overline{{}^{0^3}}\,\overline{B} + \overline{\ }\,\overline{}$$

4.2 Simple Radiative Transfer with Reynolds Decomposition

We will simplify the above example even further. In the case where the Planck Function *B* equals zero (no emission) and the Di usivity Factor *D* equals one (Radiation travels in only one direction). Equation (

new approximation, this time of order 3.

$$d\overline{}^{\,2}F^{\prime} = \quad \overline{}^{\,3}\,\overline{F} + \overline{}^{\,2}F^{\prime} + + \overline{}^{\,3}F^{\prime} \quad dz \tag{4.22}$$

Now $\overline{}^{\,3}F^{\prime}$ is an unknown.

Up to third order accuracy we can de ne F by these three equations:

$$\frac{d\overline{F}}{dz} = \quad \overline{F} \quad \overline{F^{\prime}} \tag{4.23a}$$

$$\frac{d\overline{F^{\prime}}}{dz} = \quad \overline{}^{\,2}\,\overline{F} \quad \overline{F^{\prime}} \quad \overline{}^{\,2}F^{\prime} \tag{4.23b}$$

$$\frac{d\overline{}^{\,2}F^{\prime}}{dz} = \quad \overline{}^{\,3}\,\overline{F} \quad \overline{}^{\,2}F^{\prime} \quad \overline{}^{\,3}F^{\prime} \tag{4.23c}$$

If we set $F = \overline{F}$, $G = \overline{F^{\prime}}$, $H = \overline{}^{\,2}F^{\prime}$ and $I = \overline{}^{\,3}F^{\prime}$ we obtain:

$$\frac{dF}{dz} = \quad F \quad G \tag{4.24a}$$

$$\frac{dG}{dz} = \quad \overline{}^{\,2}\,F \quad G \quad H \tag{4.24b}$$

$$\frac{dH}{dz} = \quad \overline{}^{\,3}\,F \quad H \quad I \tag{4.24c}$$

It is clear that 4.24

Again we have a closure problem as described in the previous section. The

of x, so a normal distribution of x willtionwilltg8wil8b

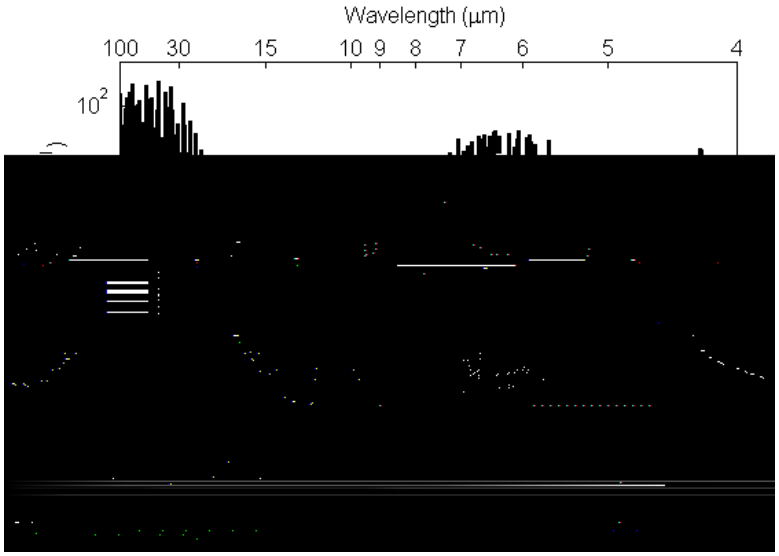

Figure 4.2: Extinction coe cient spectrum due to CO_2, H_2O and O_3 in the IR region

The extinction coe cient is measured in m^{-1} as it is a measure of the molecular absorption cross-section, per m^3 of air.

The external le also includes data for the Planck function over the wavelength spectrum shown in gure (4.3).

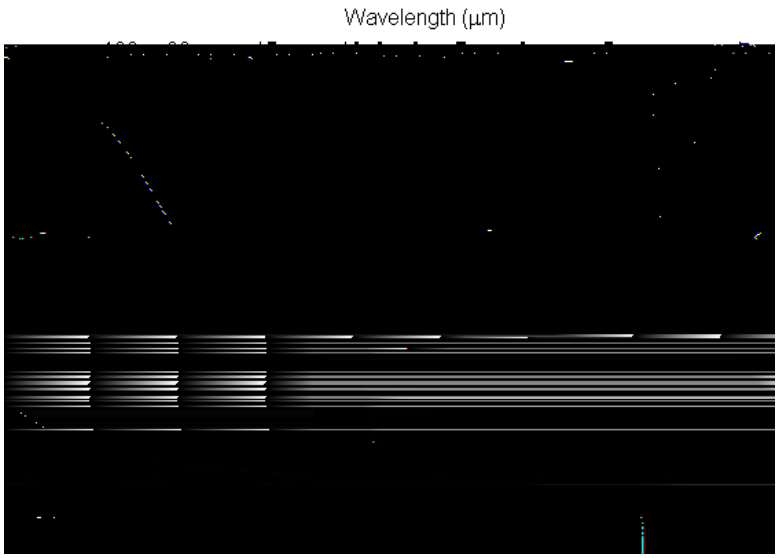

Figure 4.3: Varitation of Planck Function with wavelength and wavenumber in over IR region

Chapter 5

Results

5.1 Basic Model

5.1.1 Normal Distribution

Figure (5.1) shows the transmittance along a homogeneous path through the atmosphere. The thick black line represents the true transmittance and is equivalent to the LBL calculations. These graphs were obtained using 5000 points in z and a space step of, dz = 20.

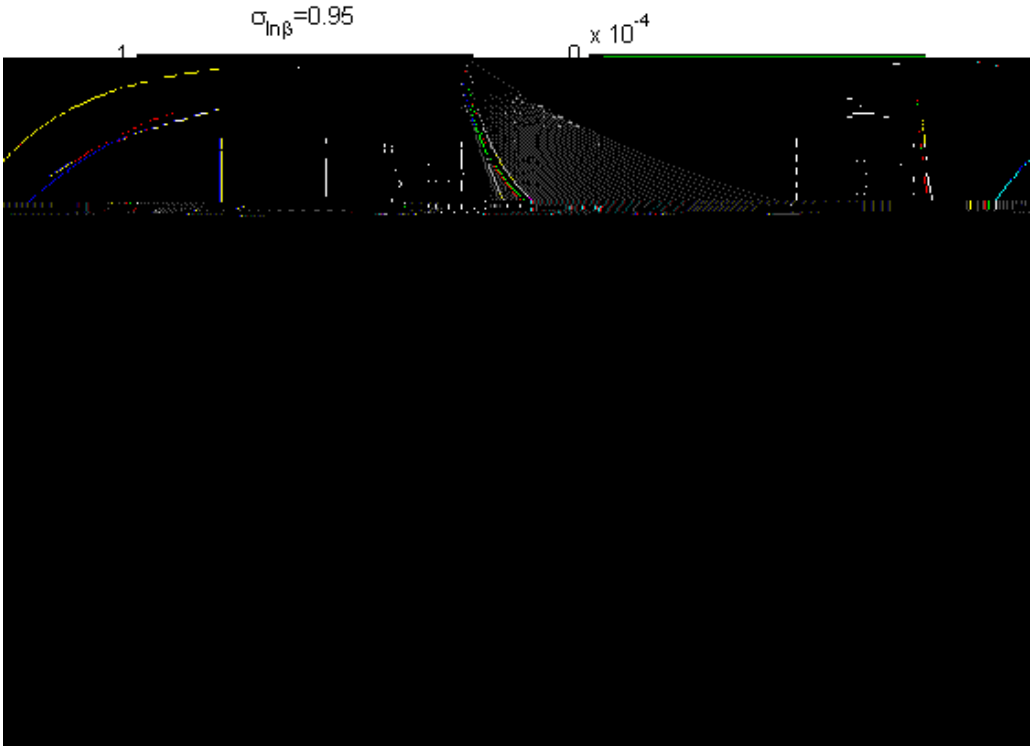

Figure 5.1: Blue = numerical rst order transmittance, red = second order numerical transmittance, green = numerical third order transmittance. Normal distribution, =0.95.

The blue line represents the numerical rst order radiative transfer when the uctuating terms are averaged across the whole spectrum. The scaling factor is 0.357 which determines the spread of the absorption coe cients, this results in a standard deviation, , of 0.95. The red line is the second order numerical transmittance and the green line is the numerical third order transmittance. The many grey lines represent the raw transmissions of each absorption coe cient. There are 61 absorption coe cients in the spectrum. It is therefore clear form gure 5.1 that the absorption coe cient spectrum is normally distributed represented by gure 5.2.

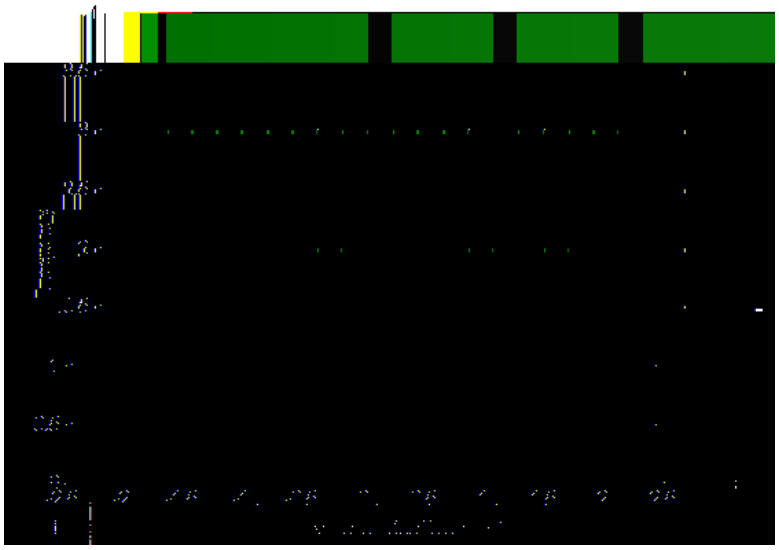

Figure 5.2: Histogram of extinction coe cients, normally distributed.

Figure 5.3

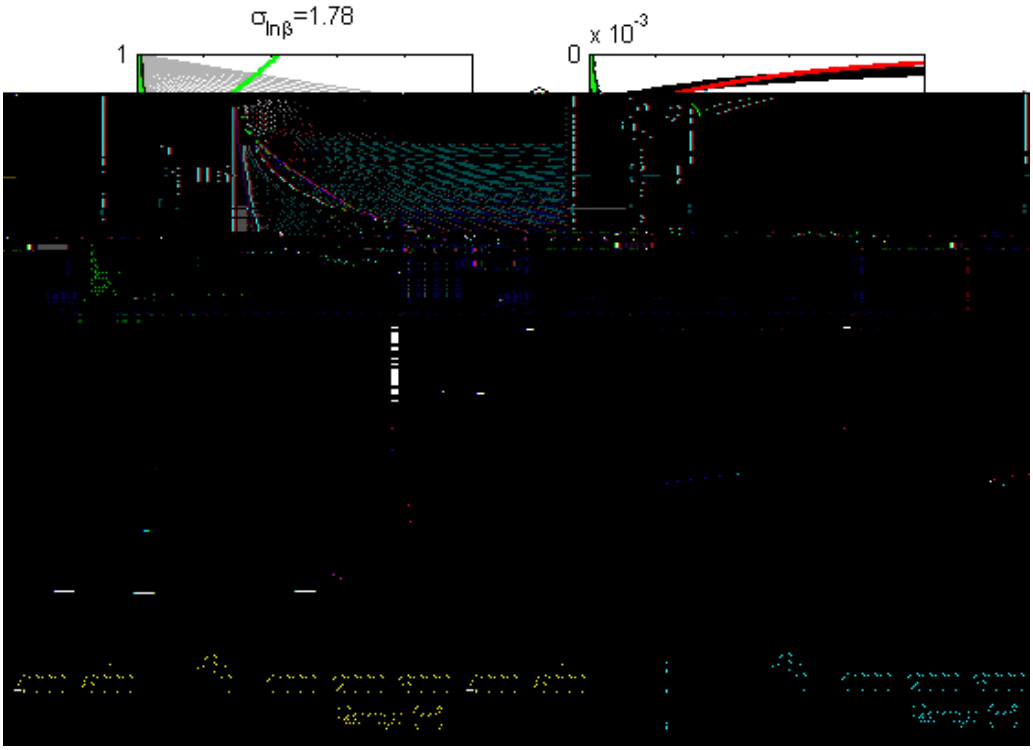

Figure 5.3: Blue = numerical first order transmittance, red = second order nu-

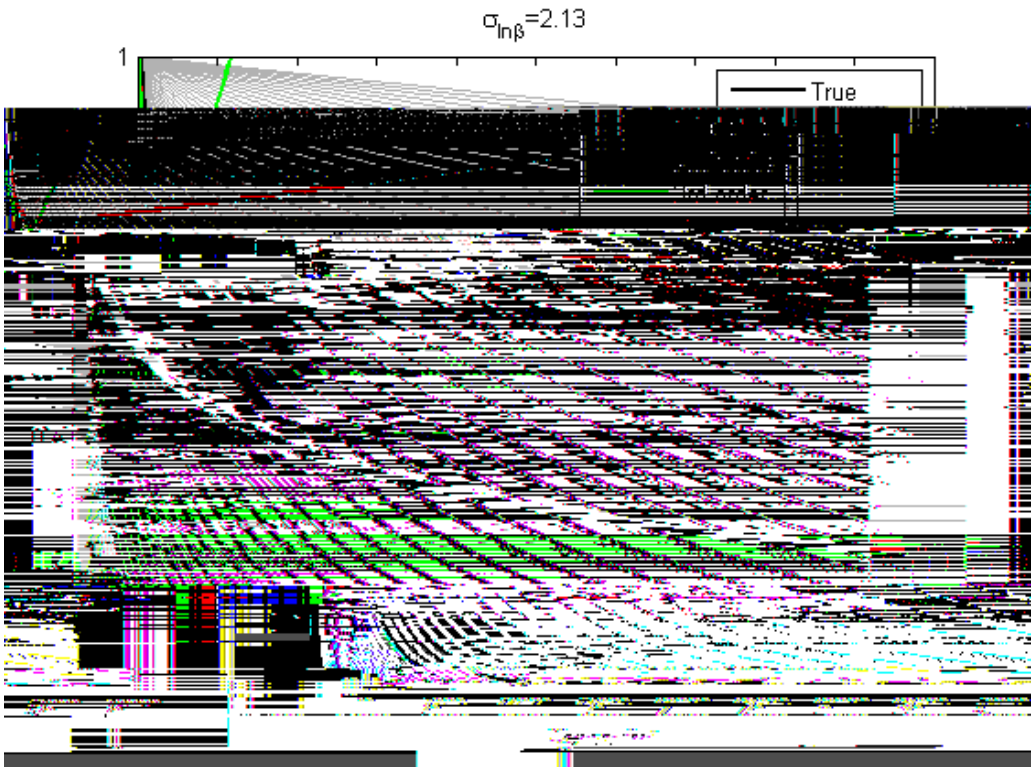

Figure 5.4: Blue = numerical rst order transmittance, red = second order numerical transmittance, green = numerical third order transmittance. Normal distribution, =2.13.

The variation in covariance has not been plotted as the third order (green)

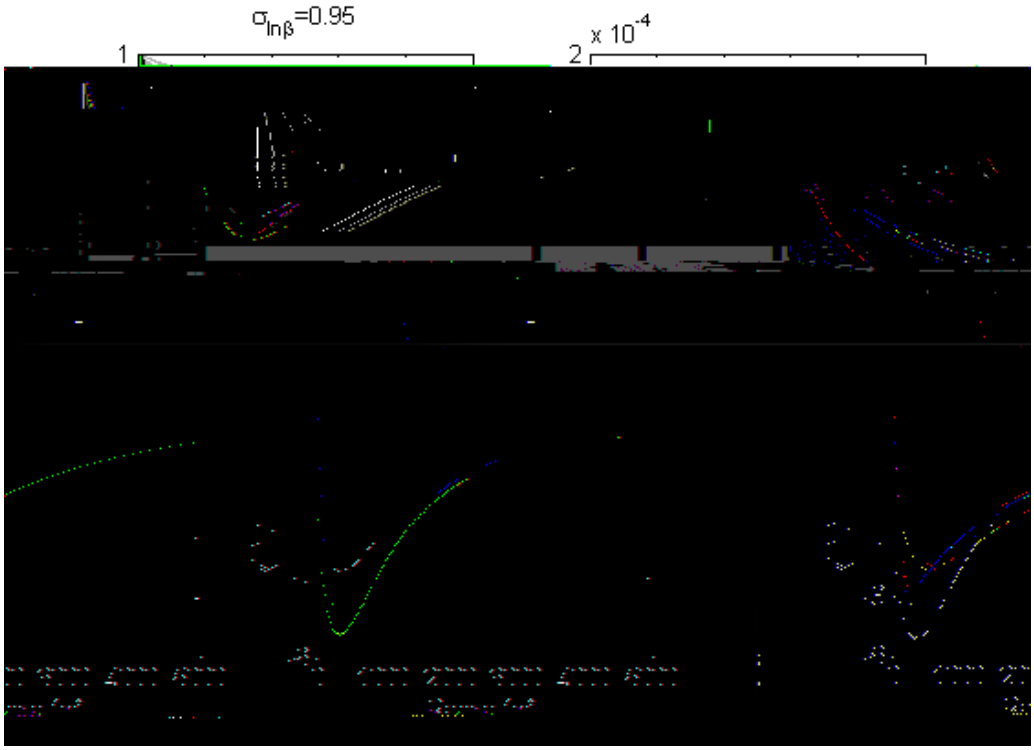

Figure 5.5: Blue = numerical first order transmittance, red = second order numerical transmittance, green = numerical third order transmittance. Gaussian distribution, =0.95.

Figure 5.5 has a scaling factor of one to achieve the standard deviation = 0.95 and also has 61 absorption coefficients in the spectrum. It is clear from the raw transmission for each individual absorption coefficient (faint grey lines) that the distribution is Gaussian, represented in figure 5.6.

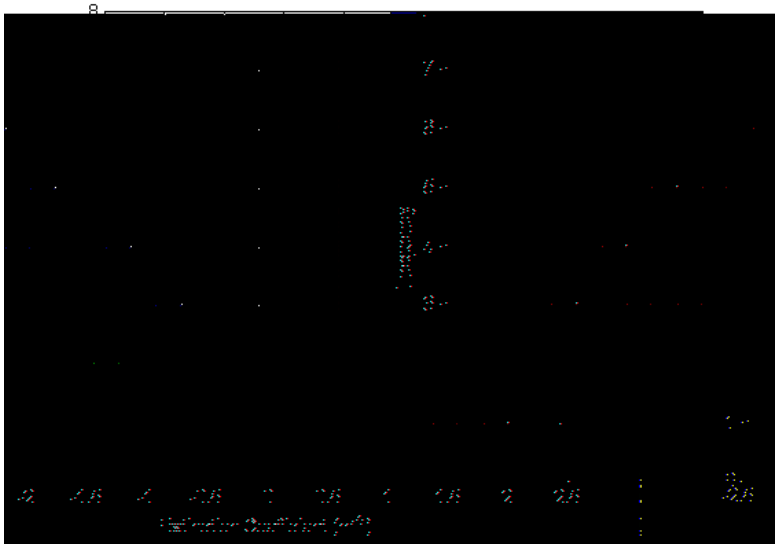

Figure 5.6: Histogram of extinction coe cients, Gaussian distributed.

It appears that for the same standard deviation in a normal distribution, g-ure 5.1 and a Gaussian distribution, gure 5.5, the Gaussian distribution is more accurate at approximating the transmittance along the path. As the distribution is Gaussian however, each time the model is run, the distribution changes. Figure 5.7 has the same standard deviation, = 0.95, as gure 5.5, yet has produced di erent approximations for each of the rst, second and third order transmissions.

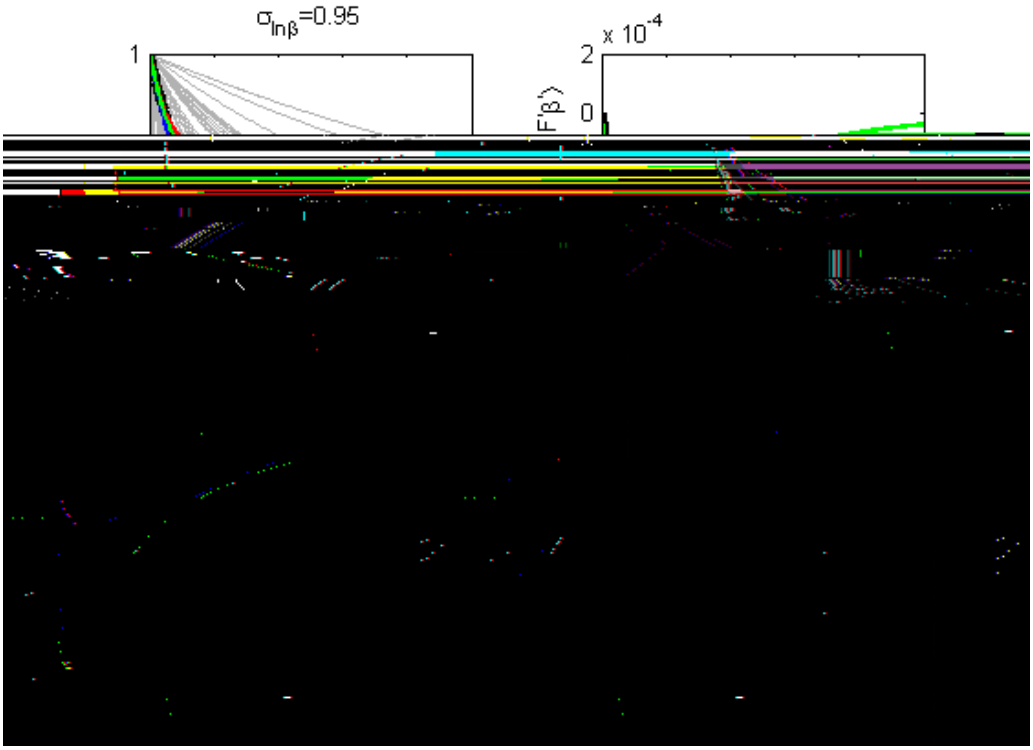

Figure 5.7: Blue = numerical rst order transmittance, red = second order numerical transmittance, green = numerical third order transmittance. Gaussian distribution, =0.95.

Figure 5.8 has a scaling factor of 1.89 to achieve the standard deviation the same as gure 5.3 yet the second order approximation has blown up very quickly and the third order transmission drops quickly to zero.

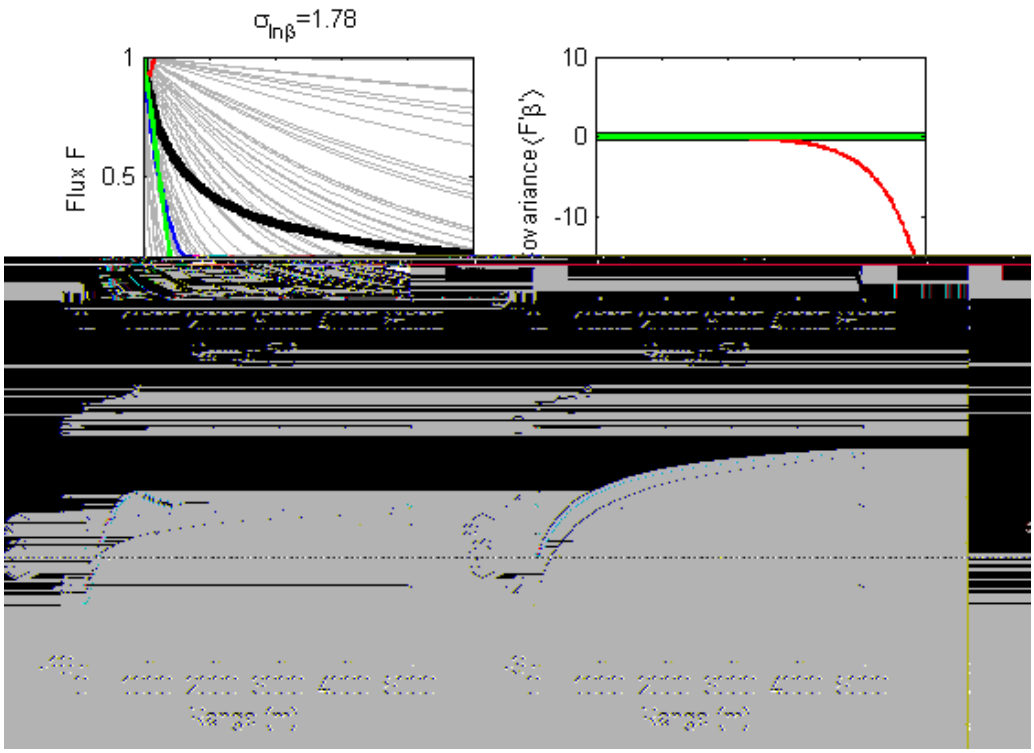

Figure 5.8: Blue = numerical rst order transmittance, red = second order numerical transmittance, green = numerical third order transmittance. Gaussian distribution, =1.78. 2imple two bandmod2l

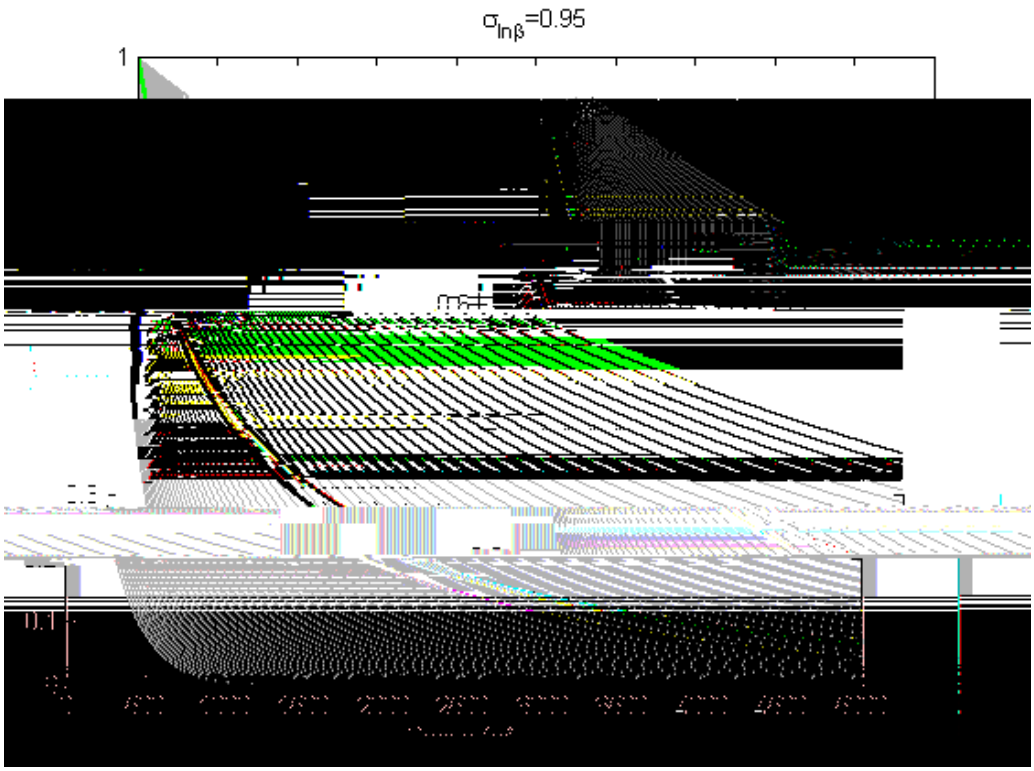

Figure 5.9: Two band model. Blue = numerical rst order transmittance, red = second order numerical transmittance, green = numerical third order transmittance. Normal distribution, =0.95.

5.2.2 Gaussian

Figure 5.10 has a Gaussian distribution of absorption coe cients and has the same standard deviation as the Gaussian distributed gure 5.5.

5.3 Equal weight band model

5.3.1 Atmospheric data

In the absorption coe cient spectrum, there are 9610 values plotted in gure 4.2. Figure 5.11 was produced sampling every single absorption coe cient. The model takes a while to run, sampling 9610 points. Figure 5.11 shows the route mean squared (RMS) accuracy of the transmission of the rst second and third order numerical approximations compared to the true transmission as the number of bands in the model is increased.

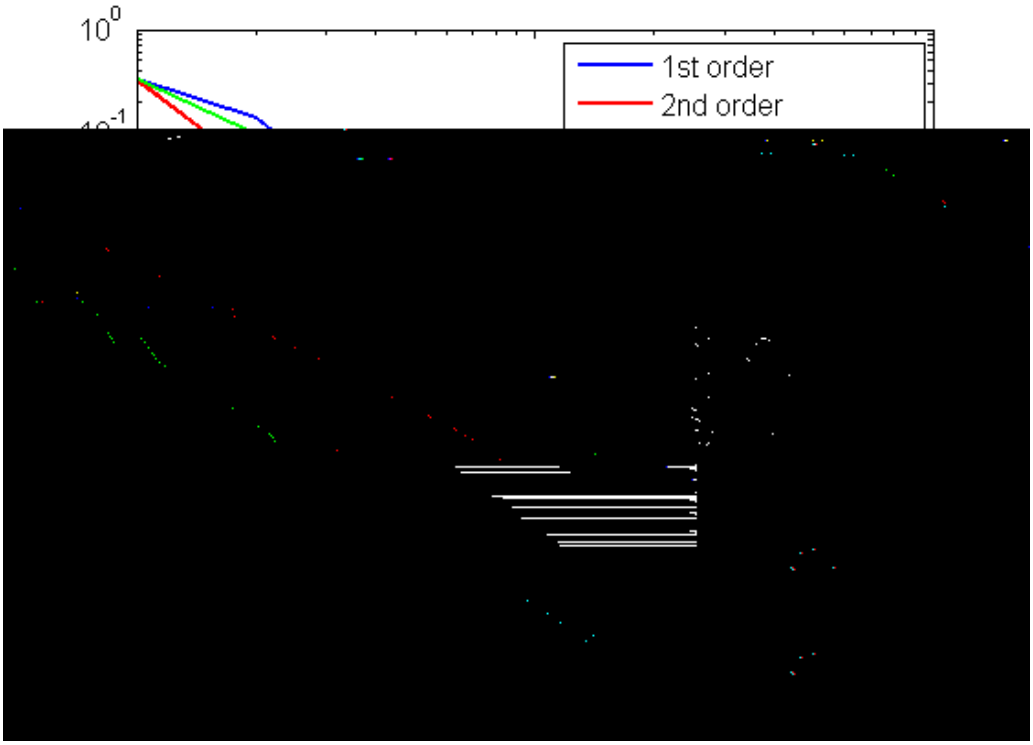

Figure 5.11: Equally weighted bands. Blue = numerical rst order transmittance RMS error, red = second order numerical transmittance RMS error, green = numerical third order transmittance RMS error, for atmospheric data.

We can however sample a smaller number of extinction coe cients such as every 30 shown in gure 5.12.

5.4.1 Atmospheric data

Figure 5.13 was produced sampling every single absorption coe cient. Figure 5.13 shows the route mean squared (RMS) accuracy of the transmission of the rst, second and third order numerical approximations compared to the true transmission as the number of bands in the model is increased.

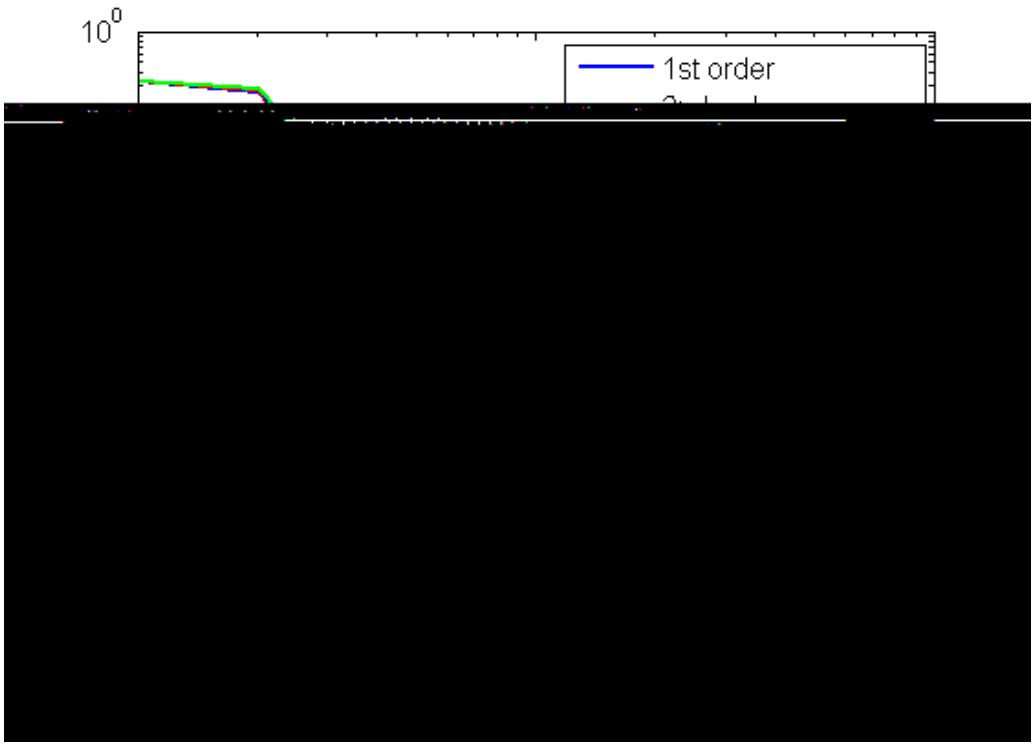

Figure 5.13: Weighted bands. Blue = numerical rst order transmittance RMS error, red = second order numerical transmittance RMS error, green = numerical third order transmittance RMS error, for atmospheric data.

Figure 5.14 was produced sampling every 20th absorption coe cient. The model samples 480 points. Already the rst order approximation is beginning to blow up. So with this technique we have to carry out a ner sample of absorption coe cient.

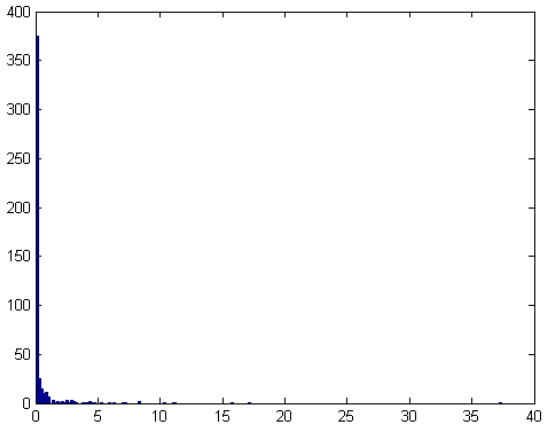

Figure 5.15: Histogram of atmospheric data extinction coe cients.

Chapter 6

Discussion

For a normal distribution of absorption coe cients and a standard deviation of, = 0.95, gure 5.1

are generate randomly, a di erent spectrum is produced each time. This can lead to a very di erent distribution with the same standard deviation, dramatically a ecting the ability to produce accurate results. This is shown by comparing gure 5.7 with gure 5.5, which have the same standard deviation, 0.95, yet they have both produced di erent approximations for each of the rst, second and third order transmissions.

In section 5.2, it is clear that by simply splitting the spectrum into two bands, the accuracy of all the three di erent schemes are better at approximating the true transmission. Both the normal and Gaussian distributions have improved their accuracy compared to performing the calculation across the whole spectrum.

Figure 5.9 samples all 9610 absorption coe cients in the atmospheric data le and represents the accuracy of the numerical schemes compared to the true transmission when the number of bands (each with the same number of absorption coe cients) is increased from one to 100. An accuracy of 10^{-6} Wm^{-2} is achieved for 100 bands. This is an acceptable error for the scheme.

It is not essential to sample the absorption coe cient at every value. Relatively good accuracy is achievable by sampling every 10 or 20, gure 5.12. In sampling the absorption spectrum more sparsely we can reduce the time taken to compute the transmission. The numerical third order approximation is the quickest to increase in accuracy as the number of bands are increased, however at around 15 bands, the accuracy levels o , the reasons why need to be investigated. The numerical second order approximation is the most accurate reaching a RMS error of 10^{-6} Wm^{-2} by 100 bands. The rst order approximation reaches an RMS error of 10^{-4} Wm^{-2} by 100 bands.

We would expect the band model in section 5.4, which has a equal fraction of the dynamic range to perform better in terms of accuracy, as a relatively larger number of lesser important (smaller absorption coe cients) are treated all together than when each band has an equal number of absorption coe cients. This means that the more important, larger absorption coe cients are treated across more bands so are considered in greater detail than in the equally weighted band model. This would appear to be disputed however as gures 5.11 and 5.12

are producing results to a greater accuracy than the equally weighted band model, gures 5.13 and 5.14.

Is is clear that the models discussed have di culty in handling a large range in extinction coe cient, this is why bands are so important and have been used throughout the development of radiative transfer models. They enable a smaller range of absorption coe cients to be considered within each band and therefore

Chapter 7

Conclusions

The next step in the development and testing of a Reynolds averaged radiative transfer model would be to include radiation travelling in di erent directions, D=1.66 and to also include emission along the path, therefore having to include the planck function. This would involve solving the systems of equations in (4.17). Then we would like to account for scattering. We would also like to account for an inhomogeneous path, where pressure and temperature change, i.e. vertically through the atmosphere, so the absorption spectrums of the gases will change due to pressure broadening.

The next step might be to develop the maths for application to shortwave atmospheric radiative transfer and ultimately to develop a radiative transfer module that may be used in operational numerical weather prediction or GCMs. Comparisons between the newly developed method and current models would be required to determine the relative accuracy of the model. The use of Reynolds decomposition within the radiative transfer equations has the potential for improving the computational requirements of the radiative transfer code relative to traditional correlated k-distribution methods.

References

Clough, S.A., Shephard, M.W., Mlawer, E.J., Delamere, J.S., Iacono, M.J., Cady-Pereira, K., Boukabara, S. & Brown, P.D. (2005). Atmospheric radiative transfer modeling: a summary of the AER codes. *Journal of Quantitative Spectroscopy Radiative Transfer*, 91, 233244.

Coelhoa, P.J., Teerling, O.J. & Roekaerts, D. (2003). Spectral radiative

Fu, Q. & Liou, N. (1992). On the Correlated k-Distribution Method for Radiative Transfer in Nonhomogeneous Atmospheres. *Journal of the Atmospheric Sciences*, 49, 2139{2156.

Hogan, R.J. (2010). The Full-Spectrum Correlated-k Method for Longwave Atmospheric Radiative Transfer Using an E ective Planck Function. *Journal of Atmospheric Sciences*, 67, 2086{2100.

Jacobson, M.Z. (2004). A Re ned Method of Parameterizing Absorption Coefcients among Multiple Gases Simultaneously from Line-by-Line Data. *Jounal of the Atmospheric Sciences*, 62, 506{517.

Lacis, A.A. & Oinas, V. (1991). A Description of the Correlated k Distribution Method for Modeling Nongray Gaseous Absorption, Thermal Emission, and Multiple Scattering in Vertically Inhomogeneous Atmospheres. *Journal of Geophysical Research*, 96, 9027{9063.

Li, G. & Modest, M.F. (2002). Application of composition PDF methods in the investigation of turbulenceradiation interactions. *Journal of Quantitative Spectroscopy Radiative Transfer*, 73, 461472.

Liou, K.N. (1992). *Radiation and Cloud Processes in the Atmosphere*. Oxford Uiversity Press, Oxford.

Mlawer, E., Traubman, S. & Clough, S. (1995). A Rapid Radiative Transfer Model. *Proceedings of the Fifth Atmospheric Radiation Measurement (ARM) Science Team Meeting*, 219{222.

Mlawer, E.J., Taubman, S.J., Brown, P.D., Iacono, M.J. & Clough, S.A. (1997). Radiative transfer for inhomogeneous atmospheres: RRTM, a validated correlated-k model for the longwavel. *Journal of Geophysical Research*, 102, 16,663{16,682.

Modest, M.F. & Zhang, H. (2002). The Full-Spectrum Correlated-k Distribution for Thermal Radiation From Molecular Gas-Particulate Mixtures. *Journal of Heat Transfer*, 124, 30{38.

Natraja, V., Jianga, X., Shiaa, R., Huangb, X., Margolisc, J.S. & Yunga, Y.L. (2005). Application of principal component analysis to high spectral resolution radiative transfer: A case study of the O_2 A band. *Journal of Quantitative Spectroscopy Radiative Transfer*, 95, 539556.

Oinas, V., Lacis, A.A., Rind, D., Shindella, D.T. & Hansen, J.E. (2001). Radiative cooling by stratospheric water vaporbig di erences in GCM results. *Journal of the AR.,.g0G/ie,s*